


Multicompartmental models and diffusion abnormalities in paediatric mild traumatic brain injury

Andrew R. Mayer,^{1,2,3,4} Josef M. Ling,¹  Andrew B. Dodd,¹ David D. Stephenson,¹ Sharvani Pabbathi Reddy,¹ Cidney R. Robertson-Benta,¹ Erik B. Erhardt,⁵ Robert L. Harms,⁶ Timothy B. Meier,^{7,8,9} Andrei A. Vakhtin,¹ Richard A. Campbell,⁴ Robert E. Sapien¹⁰ and John P. Phillips^{1,3}

The underlying pathophysiology of paediatric mild traumatic brain injury and the time-course for biological recovery remains widely debated, with clinical care principally informed by subjective self-report. Similarly, clinical evidence indicates that adolescence is a risk factor for prolonged recovery, but the impact of age-at-injury on biomarkers has not been determined in large, homogeneous samples. The current study collected diffusion MRI data in consecutively recruited patients ($n = 203$; 8–18 years old) and age and sex-matched healthy controls ($n = 170$) in a prospective cohort design. Patients were evaluated subacutely (1–11 days post-injury) as well as at 4 months post-injury (early chronic phase). Healthy participants were evaluated at similar times to control for neurodevelopment and practice effects. Clinical findings indicated persistent symptoms at 4 months for a significant minority of patients (22%), along with residual executive dysfunction and verbal memory deficits. Results indicated increased fractional anisotropy and reduced mean diffusivity for patients, with abnormalities persisting up to 4 months post-injury. Multicompartmental geometric models indicated that estimates of intracellular volume fractions were increased in patients, whereas estimates of free water fractions were decreased. Critically, unique areas of white matter pathology (increased free water fractions or increased neurite dispersion) were observed when standard assumptions regarding parallel diffusivity were altered in multicompartmental models to be more biologically plausible. Cross-validation analyses indicated that some diffusion findings were more reproducible when ~70% of the total sample (142 patients, 119 controls) were used in analyses, highlighting the need for large-sample sizes to detect abnormalities. Supervised machine learning approaches (random forests) indicated that diffusion abnormalities increased overall diagnostic accuracy (patients versus controls) by ~10% after controlling for current clinical gold standards, with each diffusion metric accounting for only a few unique percentage points. In summary, current results suggest that novel multicompartmental models are more sensitive to paediatric mild traumatic brain injury pathology, and that this sensitivity is increased when using parameters that more accurately reflect diffusion in healthy tissue. Results also indicate that diffusion data may be insufficient to achieve a high degree of objective diagnostic accuracy in patients when used in isolation, which is to be expected given known heterogeneities in pathophysiology, mechanism of injury and even criteria for diagnoses. Finally, current results indicate ongoing clinical and physiological recovery at 4 months post-injury.

- 1 The Mind Research Network/LBERI, Albuquerque, NM 87106, USA
- 2 Department of Psychology, University of New Mexico, Albuquerque, NM 87131, USA
- 3 Department of Neurology, University of New Mexico, Albuquerque, NM 87131, USA
- 4 Department of Psychiatry and Behavioral Sciences, University of New Mexico, Albuquerque, NM 87131, USA
- 5 Department of Mathematics and Statistics, University of New Mexico, Albuquerque, NM 87131, USA
- 6 Maastricht, The Netherlands
- 7 Department of Neurosurgery, Medical College of Wisconsin, Milwaukee, WI 53226, USA

8 Department of Cell Biology, Neurobiology and Anatomy, Medical College of Wisconsin, Milwaukee, WI 53226, USA

9 Department of Biomedical Engineering, Medical College of Wisconsin, Milwaukee, WI 53226, USA

10 Department of Emergency Medicine, University of New Mexico, Albuquerque, NM 87131, USA

Correspondence to: Andrew Mayer, PhD
The Mind Research Network
Pete & Nancy Domenici Hall, 1101 Yale Blvd. NE
Albuquerque, NM 87106, USA
E-mail: amayer@mrn.org

Keywords: neuroimaging; multicompartmental models; mean diffusivity; orientation dispersion index; volume fractions

Introduction

Paediatric mild traumatic brain injury (pmTBI) represents a serious public health concern based on the sheer number of youth affected each year (~750 000 cases) in the USA alone, estimated incidence of persistent post-concussive symptoms (20–35%) and the potential risk for altered developmental trajectories.^{1–3} Multiple white matter (WM) and grey matter (GM) abnormalities may exist post-injury, with each pathology exhibiting unique time-courses for recovery.^{4,5} However, systematic reviews indicate a lack of large, prospective imaging^{1,6} and biofluid⁷ studies examining the physiological effects of pmTBI. Preclinical^{8,9} and clinical (age 13 or older)³ data indicate that age-at-injury influences recovery, potentially as a result of differences in plasticity or injury during critical periods. The impact of age on more objective markers of injury remains relatively unknown due to heterogeneous sampling strategies that conflate injury severity (i.e. mild through severe TBI) and overlapping neurodevelopment periods in clinical studies.^{10,11}

Diffusion MRI (dMRI) is arguably the most widely used biomarker for investigating microstructural pathophysiology *in vivo* following pmTBI.^{1,6} Several independent studies have reported increased fractional anisotropy (FA) in the subacute (SA) stage (i.e. first days to few weeks post-injury) of pmTBI relative to both healthy (HC) and orthopaedically injured controls,^{12–16} with some studies also reporting reduced mean diffusivity (MD).^{12,13,16} Others have reported no differences,^{17–19} or reduced FA during the SA injury stage of pmTBI^{20–22} and in patients with persistent post-concussive symptoms.²³ Diffusion tensor imaging (DTI) findings are typically attributed to changes in water volume fractions (i.e. oedema), myelin or neurite structure, with a subset of studies indicating that DTI abnormalities persist beyond typical clinical recovery periods.^{14,15}

The majority of pmTBI studies so far have used a single *b*-value and assumed that diffusion occurs in a linear fashion. Microstructural abnormalities associated with trauma^{4,24} can manifest as the same DTI signal (e.g. changes in membrane structure or vasogenic oedema as reduced FA), as DTI scalars are only statistical representations (i.e. magnitude estimates) of diffusion vectors. In contrast, multi-shell acquisition schemes in conjunction with multicompartmental, geometric models of non-Gaussian diffusion can provide additional information on microstructure volume fractions that can be used to further explain underlying biological mechanisms such as oedema and microstructural integrity.^{25,26} Commonly estimated tissue volume fractions include free water and neurite density, as well as the relative dispersion of neurites.

Previous studies in adult mTBI^{27–29} suggest that Neurite Orientation Dispersion and Density Imaging (NODDI)³⁰ indices of intracellular volume fraction (V_{ic} , also commonly referred to as neurite density and used interchangeably herein), isotropic volume fraction (V_{iso} , also commonly referred to as free water and used

interchangeably herein) and orientation dispersion index (ODI) provide both statistically unique and overlapping information relative to FA and MD. However, multicompartmental models have been critiqued²⁵ for using certain constraints and/or assumptions such as fixed rates of intracellular and extracellular diffusivity at 1.7 ms/ μm^2 (NODDI),³⁰ or increased extracellular relative to intracellular diffusivity in WM (WM tract integrity model).³¹ These assumptions reduce the likelihood of degeneracy during non-linear fitting.²⁵ However, *in vivo* experiments and empirical data each suggest that intracellular parallel diffusivity is greater than extracellular diffusivity in WM and that magnitude and ratio of parallel diffusivities vary across tissue (WM > GM) classes.^{32,33} The effects of using more biologically informed (i.e. tissue-specific rates of parallel diffusivity) multicompartmental diffusion models in pmTBI remains to be investigated.

The current study therefore examined the effect of age-at-injury and subsequent recovery on traditional DTI metrics and estimated volume fractions in a large cohort of prospectively recruited pmTBI patients and age/sex-matched HC. We proposed that pmTBI would exhibit increased FA/V_{ic} and decreased MD/V_{iso} relative to HC,²⁸ that these abnormalities would persist up to 4 months post-injury¹⁴ and that abnormalities would be more evident in adolescents relative to younger children.^{3,11} It was hypothesized that volume fractions from biologically informed multicompartmental models would be more sensitive to WM pathology. Finally, we predicted that more objective injury characteristics [loss of consciousness (LOC)] and post-traumatic amnesia (PTA) would be associated with dMRI abnormalities whereas self-reported post-concussive symptoms (PCS) and clinical risk scores³ would not account for significant variance at current sample sizes due to anticipated smaller effect sizes.^{19,34,35}

Materials and methods

Participants

Patients (8–18 years of age) were consecutively recruited from local emergency department and urgent care settings between July 2016 and February 2020 in this prospective cohort design (Fig. 1). Data collection occurred during SA (1–11 days post-injury) and early chronic (EC, ~4 months post-injury) injury phases. Inclusion criteria were based on both American Congress of Rehabilitation Medicine (upper threshold)³⁶ and Zurich Concussion in Sport Group (lower threshold),³⁷ and included Glasgow Coma Score ≥ 13 , LOC (if present) limited to 30 min, PTA (limited to 24 h), alteration in mental status at the time of injury or at least two new PCS. HC were recruited to match based on age and sex, and assessed at identical time intervals to control for neurodevelopmental confounds and/or repeat assessment.

Exclusion criteria for both groups included history of (i) previous TBI with >30 min LOC; (ii) neurological diagnosis; (iii) psychiatric disorders other than adjustment disorder; (iv) developmental disorders (autism spectrum disorder or intellectual disability); (v) history of substance abuse/dependence; (vi) contraindications for MRI including pregnancy; and (vii) non-English speaking. Patients were excluded if general anaesthesia was administered during hospitalization, or for injury to the dominant hand. Additional exclusion criteria for HC included Attention-Deficit Hyperactivity Disorder or learning disability diagnoses. A positive urine test also resulted in exclusion. The study was approved by the University of New Mexico Institutional Review Board and informed consent/assent was obtained based on the Declaration of Helsinki.

The final SA sample ([Supplementary material](#) and [Fig. 1](#)) included 204 pmTBI (83 females; age 14.5 ± 2.9 ; 7.4 ± 2.2 days post-injury) and 173 matched HC (73 females; age 14.2 ± 2.8). A total of 152 pmTBI (63 females; 130.9 ± 14.5 days post-injury; 124.0 ± 14.6 days between visits; 81.3% retention without individuals excluded from study) and 155 HC (65 females; 124.2 ± 15.7 days between visits; 95.5% retention without study excludes) returned for the second visit.

Clinical assessments

A Common Data Elements battery of primary and secondary measures ([Supplementary material](#) and [Supplementary Table 1](#)) was administered at both visits, with retrospective ratings of symptoms (i.e. 1 month before) also acquired when possible. Measures included previous medical history, the New Mexico Assessment of Pediatric Traumatic Brain Injury semi-structured interview,³⁸ the Alcohol, Smoking and Substance Involvement Screening Test,³⁹ self and parent reports of concussion symptom severity (Post-Concussion Symptom Inventory),^{40,41} Patient Reported Outcomes Measurement Information System for sleep,⁴² anxiety and depression,⁴³ a brief pain rating (0–10 Likert scale),⁴⁴ self-report of Tanner stage of development,⁴⁵ Headache Impact Test (HIT-6),⁴⁶ the Strengths and Difficulties Questionnaire,⁴⁷ Conflict and Behavioral Questionnaire,⁴⁸ Pediatric Quality of Life Inventory (PedsQL-Generic Core)⁴⁹ and the Glasgow Outcome Scale Extended (GOS-E) Pediatric Revision.⁵⁰ Parental distress was measured with the Brief Symptom Inventory (BSI-18).⁵¹ A modified version of the 5P risk score⁵² was calculated on the basis of available clinical data ([Supplementary material](#)). A binary indication of symptomatic versus asymptomatic PCS status was calculated using HC data and published methods ([Supplementary material](#)).⁵³ Estimates of reading ability and effort were obtained,⁵⁴ as well as primary (attention and processing speed) and secondary (working memory, executive functioning and long-term memory recall) cognitive domains ([Supplementary material](#)).

Image acquisition

High resolution T₁-weighted (voxel size = 1.0 mm³), T₂-weighted (voxel size = 1.15 × 1.15 × 1.5 mm), susceptibility-weighted (voxel size = 1.0 × 1.0 × 1.5 mm) and fluid-attenuated inversion recovery (voxel size = 0.8 × 0.8 × 3 mm) images were collected on a Siemens 3 T TrioTim scanner with a 32-channel head coil. High angular resolution dMRI scans were acquired using a twice-refocused spin-echo sequence with 165 diffusion-weighted gradients (55 each at $b = 800$ s/mm², $b = 1600$ s/mm², $b = 2400$ s/mm²) and the $b = 0$ experiment repeated eight times (72 interleaved slices; repetition time = 4000 ms; echo time = 108 ms; flip angle = 84°; refocus flip angle = 157°; number of excitations = 1; voxel resolution = 2.0 × 2.0 × 2.0 mm; field of view = 224 mm; multi-band factor = 3). Full details on imaging sequences are presented in the [Supplementary material](#). Structural magnetic resonance images

were reviewed by a board-certified neuroradiologist blinded to participant group and rated for pathology.⁵⁵ A subset of pmTBI participants ($n = 99$) received CT scans as part of routine care.

Image processing

MRI and dMRI data were preprocessed using AFNI (v.20.0.51), FSL (v.6.0.4) and SPM (v.12). Susceptibility artefacts (using reverse phase-encoded images), eddy currents and head motion were first corrected using FSL TOPUP and EDDY.⁵⁶ Data from all three shells were used for non-linear DTI calculations with AFNI.⁵⁷ The NODDI algorithm (MATLAB v.2020a)³⁰ was used with all default parameters (isotropic diffusivity = 3.0×10^{-3} mm²/s, intracellular diffusivity = 1.7×10^{-3} mm²/s, extracellular diffusivity = 1.7×10^{-3} mm²/s). Biologically informed multicompartmental models (code presented in Appendix A of the [Supplementary material](#)) were also computed using the python-based Microstructure Diffusion Toolbox (MDT, v.1.2.6).²⁶ For these models, isotropic diffusivity remained fixed (3.0×10^{-3} mm²/s) but separate diffusivity magnitudes and constraints were set for WM and GM based on existing literature.^{25,32,33} Specifically, intracellular diffusivity was fixed at 1.7×10^{-3} mm²/s for WM, whereas extracellular diffusivity was constrained to be $<1.7 \times 10^{-3}$ mm²/s. For GM, intracellular diffusivity was fixed at 1.2×10^{-3} mm²/s, whereas extracellular diffusivity was unconstrained.

Statistical analysis

Primary and secondary clinical data were assessed using age at first visit (unit = months; equivalent to age-at-injury) as a covariate, as well as retrospective ratings when applicable ([Supplementary Table 1](#)). Clinical analyses were conducted with either generalized linear models (Group effect only) or generalized estimating equations (Group and Visit effect), using Gaussian, gamma or negative binomial distributions and were Bonferroni-corrected. Voxel-wise dMRI analyses (AFNI's 3dLME module) were conducted with 2 × 2 [Group (HC versus pmTBI) × Visit (SA versus EC)] mixed factor models, with age-at-injury and mean framewise displacement entered as additional covariates, and subject intercept treated as a random effect. Voxel-wise diffusion results were corrected using both parametric ($P \leq 0.001$) and minimum volume thresholds based on latest recommendations.⁵⁸ Clinical and imaging results are reported for main effects of Group, Group × Visit, Group × Age and Group × Visit × Age interactions. Finally, a random forests approach^{59,60} was used to determine classification accuracy from both clinical and dMRI data ([Supplementary material](#)).

Data availability

The data that support the findings of this study will be openly available in FITBIR at fitbir.nih.gov, reference number FITBIR-STUDY0000339 at the conclusion of this study.

Results

Demographics

The pmTBI and HC groups did not differ in terms of handedness, age, self-reported Tanner stage of development and biological sex (all P -values ≥ 0.429 ; see [Supplementary Table 2](#)). Conversely, significant group differences were observed for self-reported history of previous head injuries ($\chi^2 = 8.96$, $P = 0.003$; pmTBI = 17.2%, HC = 6.9%), parental self-reported psychopathology (BSI-18; Wald- $\chi^2 = 12.73$; $P \leq 0.001$; pmTBI > HC), maximum parental education (Wald- $\chi^2 = 48.06$; $P \leq 0.001$; pmTBI < HC), premorbid reading ability [Wide Range

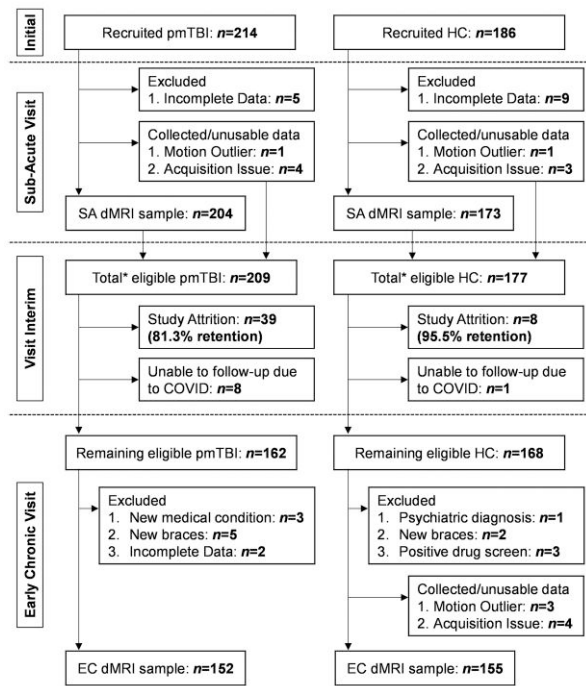


Figure 1 Participant recruitment and retention. Flowchart of enrolment, inclusion and data quality control from the SA and EC phases of injury for patients with a pmTBI, as well as matched HC. The asterisk denotes the total number of participants who were eligible to return, which is the sum of participants with usable dMRI data and those with quality assurance issues.

Achievement Test 4 (WRAT4); Wald- $\chi^2 = 29.11$; $P \leq 0.001$; pmTBI < HC] and effort [Test of Memory Malinger—10-item short version (TOMMe10); Wald- $\chi^2 = 19.38$; $P \leq 0.001$; pmTBI < HC]. The latter two measures were therefore included as additional covariates for neuropsychological analyses.

Clinical measures

Table 1 presents all clinical and neuropsychological results. A significant Group \times Visit \times Age (Wald- $\chi^2 = 6.30$; $P = 0.012$) interaction for self-reported PCS severity was observed. Follow-up tests conducted at each visit indicated a significant Group \times Age interaction in PCS severity at the SA (36.8% pmTBI symptomatic; Wald- $\chi^2 = 25.76$; $P = 0.005$) but not EC (15.8% pmTBI symptomatic; $P = 0.700$) visit. Significant group effects ($P < 0.002$; pmTBI > HC) were observed at both visits, but were larger at the SA visit. A positive association was observed at SA between PCS and age for pmTBI ($\beta = 0.061$; Wald- $\chi^2 = 5.79$; $P = 0.016$) with a negative association for HC ($\beta = -0.096$; Wald- $\chi^2 = 19.60$; $P < 0.001$). A significant Group \times Visit \times Age interaction (Wald- $\chi^2 = 6.50$; $P = 0.011$) also existed for self-reported behavioural disturbances (Conflict Behavior Questionnaire), but follow-up tests at the Visit level were not significant for Group \times Age interactions (all P -values ≥ 0.05). Trend differences in behavioural problems (pmTBI > HC) were present at the EC ($P = 0.072$) but not SA ($P = 0.446$) visit. There were no significant group effects or interactions for the primary measure of quality of life (all Bonferroni-corrected P s > 0.0167).

Secondary clinical measures (Bonferroni correction $0.05/7 = 0.007$) indicated Group \times Visit interactions for anxiety, sleep, pain and headaches (all P -values ≤ 0.007), characterized by increased symptoms (pmTBI > HC) at the SA visit (all P -values ≤ 0.001). There

were no group-wise differences for anxiety, pain and headache (all P -values > 0.05) at the EC visit. Sleep complaints were still increased for pmTBI but at a lower level relative to the SA visit ($P = 0.008$). Main effects of group (worse outcomes for pmTBI) were observed for secondary measures of depression, a parent-rated multi-dimensional measure of behavioural functioning (Strengths and Difficulties Questionnaire) and trauma-related functional outcome (GOS-E, all P -values ≤ 0.001).

Cognitive testing

Significant Group \times Visit interactions were observed for the primary cognitive domains of attention (Wald- $\chi^2 = 7.39$; $P = 0.007$) and processing speed (Wald- $\chi^2 = 6.44$; $P = 0.011$) after controlling for effort and reading ability. Simple effects testing indicated worse performance at the SA visit for pmTBI relative to HC (all P -values < 0.01) coupled with statistically equivalent performance at follow-up (all P -values > 0.05). Secondary cognitive analyses indicated Group effects (HC > pmTBI) for executive functioning ($P = 0.004$) and long-term memory recall ($P < 0.001$). There were no significant Group effects or interactions for working memory (all Bonferroni-corrected P -values > 0.0167).

Structural imaging findings

A total of 8/99 patients had positive day-of-injury CT scans for intracranial pathology or skull fracture. Four more pmTBI with negative CT scans were diagnosed with additional findings on their MRI scans that were probably related to trauma.⁵⁵

Overall relationships between dMRI measures

Secondary analyses (Supplementary Table 3 and Supplementary Fig. 1) confirmed that similar statistical relationships existed between the NODDI volume fractions and DTI metrics in healthy adolescents as previously reported for adults.²⁸ This included a very strong relationship between ODI and FA as indicated by R^2 values,²⁸ with more moderate relationships between other metrics. However, the magnitudes of relationships with DTI scalars were significantly changed when using volume fractions from the more biologically informed composite model in MDT (Supplementary Table 3 and Supplementary Fig. 2), including both decreased (FA with ODI in both GM and WM; MD and V_{ic} in GM) and increased (FA with V_{ic} in WM) R^2 values. Surprisingly, there were only small/moderate relationships between NODDI and biologically informed MDT volume fraction estimates with the exception of V_{iso} (Supplementary Table 4 and Supplementary Figs 3 and 4).

DTI findings

A significant Group \times Visit \times Age (Wald- $\chi^2 = 13.60$; $P < 0.001$) interaction existed for mean framewise displacement. A significant negative relationship existed between age and framewise displacement SA ($\beta = -0.026$; $P < 0.001$), whereas the Group \times Age interaction was significant at the EC visit (Wald- $\chi^2 = 10.53$; $P = 0.001$). This interaction resulted from a negative relationship between age and FD for pmTBI ($\beta = -0.031$; $P < 0.001$) but not HC ($P = 0.283$). Framewise displacement was therefore used as a covariate for all dMRI analyses.

Voxel-wise results of MD indicated a Group \times Visit \times Age interaction (Fig. 2A and D) within left cerebellar lobule V/VI (1393 μ l). Follow-up analyses indicated a significant Group \times Age interaction SA (Wald- $\chi^2 = 4.63$; $P = 0.031$), with a main effect of Group at the EC visit (Wald- $\chi^2 = 6.55$; $P = 0.011$; HC > pmTBI). The SA interaction resulted from a

Table 1 Clinical and neuropsychological data

Metric	Outcome	SA pmTBI (n = 204)	SA HC (n = 173)	EC pmTBI (n = 152)	EC HC (n = 155)
Symptom measures					
PCSI (% max) ^{a,b}	P	13.9 (4.8–34.9)	2.9 (0–8.8)	4.8 (0–15.5)	3.2 (0.8–8.7)
PROMIS Sleep ^a	S	19 (13.5–24)	13 (11–16)	18 (12–23)	14 (11–17)
PROMIS Anxiety ^a	S	3 (0–8)	1 (0–4)	2 (0–6.5)	1 (0–5)
PROMIS Depression ^c	S	2 (0–8)	0 (0–3)	1 (0–6)	1 (0–3)
Pain Scale ^a	S	3 (1–5)	0 (0–1)	0 (0–2)	0 (0–1)
HIT-6 ^a	S	52 (44–59)	40 (36–46.5)	44 (40–55)	42 (38–47)
Behavioural and outcome measures					
CBQ ^{a,b}	P	1 (0–2)	1 (0–2)	1 (0–3)	1 (0–2)
PedsQL	P	–	–	85.9 (75.5–94.0)	90.2 (82.6–95.7)
SDQ ^c	S	–	–	7 (4–10)	4 (2–8)
GOS-E ^c	S	1.5 (1–4)	1 (1–1)	1 (1–2)	1 (1–1)
Cognitive measures					
TOMMe10 ^c	S	10 (9–10)	10 (10–10)	10 (10–10)	10 (10–10)
WRAT4 ^c	S	49.0 (43.3–54.7)	54.7 (48.0–62.7)	49.3 (44.0–56.7)	55.3 (49.3–62.7)
PS ^a	P	46.8 ± 7.6	50.5 ± 8.1	50.3 ± 8.5	52.3 ± 8.8
AT ^a	P	47.8 (42.2–53.3)	52.2 (46.7–55.6)	50 (44.5–55.5)	52.2 (47.8–56.7)
WM	S	46.8 ± 8.0	50.4 ± 10.6	48.3 ± 9.5	50.5 ± 11
EF ^c	S	47.2 ± 7.1	50.5 ± 6.7	50.4 ± 6.8	52.9 ± 6.3
HVLT Delay ^c	S	8 (6–10)	9 (7–10)	7 (6–9)	9 (7–10)

Data are either formatted at mean ± standard deviation or median (interquartile range). AT = attention; CBQ = Conflict Behavior Questionnaire; EF = executive function; HVLT Delay = Delayed recall on Hopkins Verbal Learning Task (measure of long-term memory); PCSI = Post-Concussion Symptom Inventory (presented as percent of maximum score to account for age-related scale differences); PROMIS = Patient Reported Outcomes Measurement Information System; PS = processing speed; SDQ = Strengths and Difficulties Questionnaire; WM = working memory.

^aGroup × Visit interaction.

^bGroup × Age or Group × Visit × Age interaction.

^cGroup main effect.

negative association between MD and age for HC ($\beta = -0.003$; $P = 0.003$) that was absent for pmTBI ($P = 0.635$). Regions of decreased MD (Fig. 2B and E; HC > pmTBI) were observed in the right insula/superior temporal gyrus (BAs 13/22; 1517 μl), right superior temporal/supramarginal gyrus (BAs 13/40/41; 1340 μl), right post-central gyrus (BAs 2–5; 1549 μl), left fusiform gyrus (1590 μl), left visual cortex/cuneus (BAs 17/18; 1448 μl) and the right (BAs 7/19; 2790 μl) and left (BAs 7/19; 3058 μl) precuneus/cuneus. A single cluster (3853 μl) encapsulating grey/white junctions between the left thalamus and internal capsule, as well as between the cerebellar peduncles, brainstem and Lobules I–IV of the cerebellum, also exhibited evidence of decreased MD.

No significant voxel-wise interactions (factors of Group, Age or Visit) existed for FA. A main effect of increased FA for pmTBI relative to HC (Fig. 2C and F) was present in the bilateral visual cortex and cuneus (BAs 17/18/23/30; 1950 μl).

NODDI findings

No significant voxel-wise interactions (factors of Group, Age or Visit) existed for V_{iso} , V_{ic} or ODI.

A main effect of Group (Fig. 3A and C) characterized by decreased V_{iso} (HC > pmTBI) was observed in the right post-central gyrus (BAs 2–5; 1413 μl), right superior parietal lobule (BA 7; 1225 μl), right precuneus/cuneus (BAs 7/19; 1458 μl) and the left superior parietal lobule/precuneus/cuneus (BAs 7; 1554 μl). Qualitative comparisons of Fig. 2C and Fig. 3A and B indicate that most of the significant GM regions for NODDI V_{iso} also exhibited significant group effects in the MD analyses.

A main effect of increased V_{ic} (Fig. 4A, C and E) was also observed for pmTBI in the right temporal pole (BAs 38; 1351 μl), right inferior/middle temporal gyrus and inferior longitudinal fasciculus (BA 21; 5075 μl), along the grey/white junction of the right inferior temporal/fusiform gyrus with the inferior longitudinal/vertical

occipital fasciculus (BA 37; 2775 μl), left fusiform gyrus (BA 37; 1237 μl), left middle occipital gyrus (BA 19/37/39; 1234 μl) and the bilateral precuneus extending into the right posterior cingulate (BA 18/31; 1450 μl).

There were no significant main effects observed with NODDI estimates of ODI.

MDT findings

Similar to the NODDI model, there were no significant voxel-wise interactions (factors of Group, Age or Visit) for the biologically informed MDT measurements of V_{ic} , V_{iso} or ODI.

Only minor differences in the main effect of Group existed between NODDI and MDT estimates of V_{iso} for GM (Fig. 3B and D). Specifically, decreased V_{iso} was again observed for pmTBI in the right post-central gyrus and inferior parietal lobule (BAs 2–5/40; 3848 μl), right superior parietal lobule (BA 7; 1490 μl), right precuneus/cuneus (BAs 7/19; 1328 μl) and left superior parietal lobule/precuneus/cuneus (BAs 7/19; 1968 μl). However, clusters of increased V_{iso} (pmTBI > HC) were present in WM for the MDT model within the right anterior corona radiata (1108 μl), as well as within the right superior longitudinal fasciculus, internal and external capsule extending into the putamen (1952 μl).

The biologically informed MDT model resulted in improved sensitivity for detecting changes in V_{ic} (Fig. 4B). Spatially overlapping areas clusters of increased V_{ic} (pmTBI > HC) were observed in the right parahippocampal/fusiform gyrus (BA 37; 1711 μl) and right fusiform gyrus (BA 37; 1155 μl) in the NODDI (Fig. 4C) and MDT (Fig. 4D) models. The right superior/middle temporal gyrus also showed overlapping increased V_{ic} for pmTBI (BAs 20/21; 9206 μl) but extended further into adjoining inferior longitudinal and uncinate fasciculi. The MDT model also indicated multiple other unique areas of increased V_{ic} for pmTBI relative to the NODDI model in

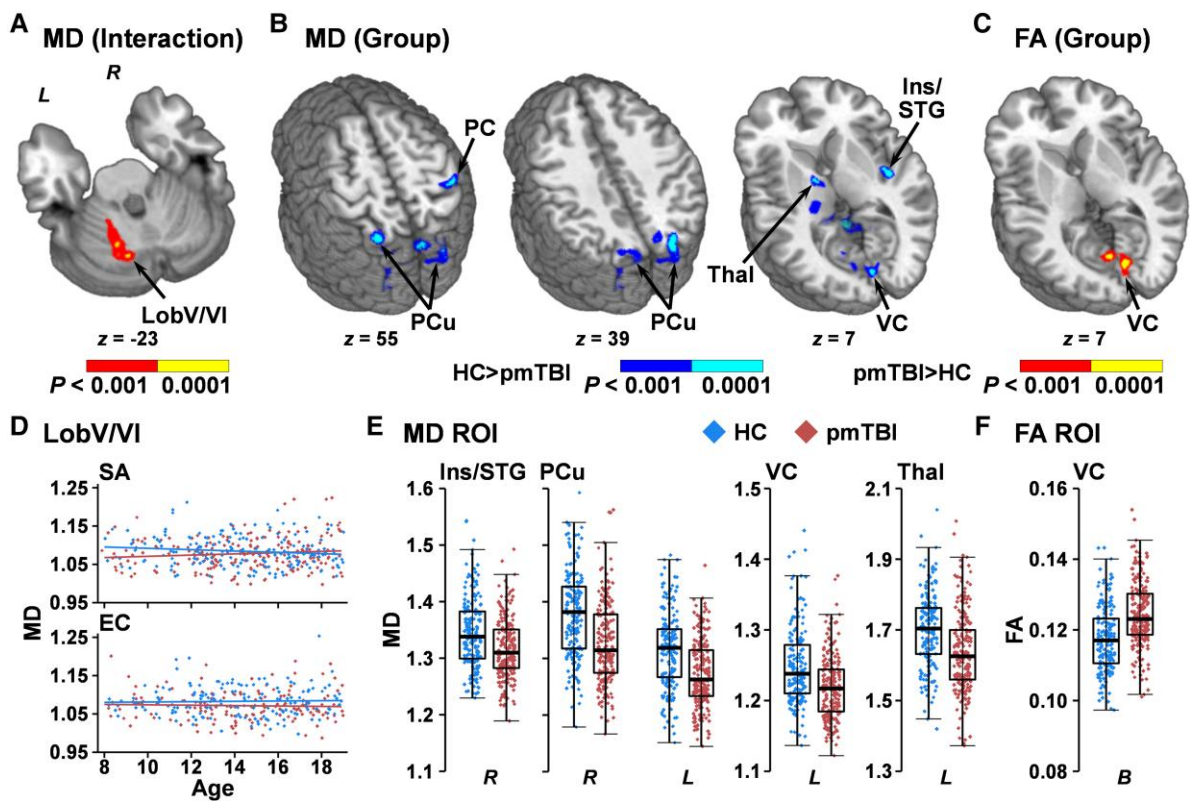


Figure 2 Voxel-wise analyses of traditional dMRI metrics. Results from the analysis of MD and FA for patients with pmTBI (red diamonds) and HC (blue diamonds). (A) A cluster within the left cerebellar Lobule V/VI that exhibited a Group \times Visit \times Age interaction (red: $P < 0.001$; yellow: $P < 0.0001$) for MD. Plotted data (D) indicate a significant negative association between residualized MD and age at the SA visit for HC, which was not significant at the EC visit. (B) The regions that demonstrated main effects of Group for MD (HC $>$ pmTBI) are displayed in cool colours (dark blue: $P < 0.001$; cyan: $P < 0.0001$), with (E) presenting box-and-scatter plots [elements: median, interquartile range (IQR) and $3 \times$ IQR or local maxima/minima] for selected regions of interest (ROIs) [post-central gyrus (PC), precuneus (PCu), insula extending into superior temporal gyrus (Ins/STG), visual cortex (VC), and thalamus (Thal)] for both right (R) and left (L) hemispheres. (C) The bilateral (B) VC was associated with increased FA for pmTBI (red: $P < 0.001$; yellow: $P < 0.0001$), with (F) presenting the box-and-scatter plot. Locations of the axial (z) slices for all panels are given according to the Talairach atlas.

cortical GM, subcortical GM, cerebellum and WM (full listing in [Supplementary material](#)) (Fig. 4F).

In contrast to the null NODDI findings, the biologically informed MDT model indicated increased ODI for pmTBI patients (Fig. 5) within the right anterior corona radiata/inferior fronto-occipital fasciculus extending into orbitofrontal cortex (BAs 11/47; 2439 μ l), the grey/white junction of the left inferior temporal gyrus with the inferior longitudinal fasciculus (BA 20; 823 μ l), the left fusiform gyrus/lobule VIIa of the cerebellum (BA 20/36; 812 μ l), the right posterior external capsule/fornix extending into the parahippocampal gyrus (BA 28; 2560 μ l), the left external capsule/fornix extending into the parahippocampal gyrus (BA 13; 3881 μ l), the left superior cerebellar peduncle extending into Lobules I–VI (4272 μ l) and the right cerebellar Lobules VI/VIIIa/VIIIb/IX (980 μ l).

Effect size estimates and reproducibility of findings

Calculated voxel-wise Cohen's d effect sizes maps were generally in the small to medium range for both DTI and biologically informed MDT metrics ([Supplementary Figs 5–8](#)).

Cross-validation analyses examined the reproducibility of imaging findings. Specifically, DTI and MDT analyses were repeated (300 iterations) at reduced sample sizes (50, 60 and 70% of total sample) without replacement. Voxels exhibiting a main effect of Group (uncorrected P -values of 0.01 due to repeated tests) were then summed and divided by the total number of iterations. Reproducibility was excellent ($>80\%$)

for most significant regions at 70% (142 pmTBI, 119 HC) of the total sample size for both DTI metrics ([Supplementary Fig. 9](#)) and the biologically informed MDT algorithm (Fig. 6). Of interest, the cerebellar peduncles, superior corona radiata, internal and external capsule demonstrated highly reproducible Group effects of increased V_{iso} in the 70% sample analyses that were either absent (peduncles) or right lateralized in the full sample due to spatial volume requirements for family-wise error corrections. However, reproducibility decreased at the 60% (122 pmTBI, 103 HC) sample size and became poor to moderate when only 50% (102 pmTBI, 85 HC) of the sample was used.

dMRI abnormalities and clinical correlations

Our final set of analyses examined the relationship between clinical indices of injury severity ([Supplementary Table 5](#)) and dMRI abnormalities in pmTBI only, as well as classification accuracy of dMRI abnormalities relative to clinical gold standards. A weighted average was calculated from all of the significant clusters in the five primary patterns showing differences between pmTBI and HC (individual patterns of decreased GM V_{iso} , increased WM V_{iso} , increased V_{ic} and increased ODI in the biologically informed MDT model, and FA). MD (overlap with GM V_{iso}) and NODDI results were excluded to eliminate redundancies.

As predicted, results ([Supplementary Table 5](#); uncorrected for multiple comparisons) indicated that LOC was positively associated with both V_{ic} ($P = 0.007$) and WM V_{iso} ($P = 0.005$) in the

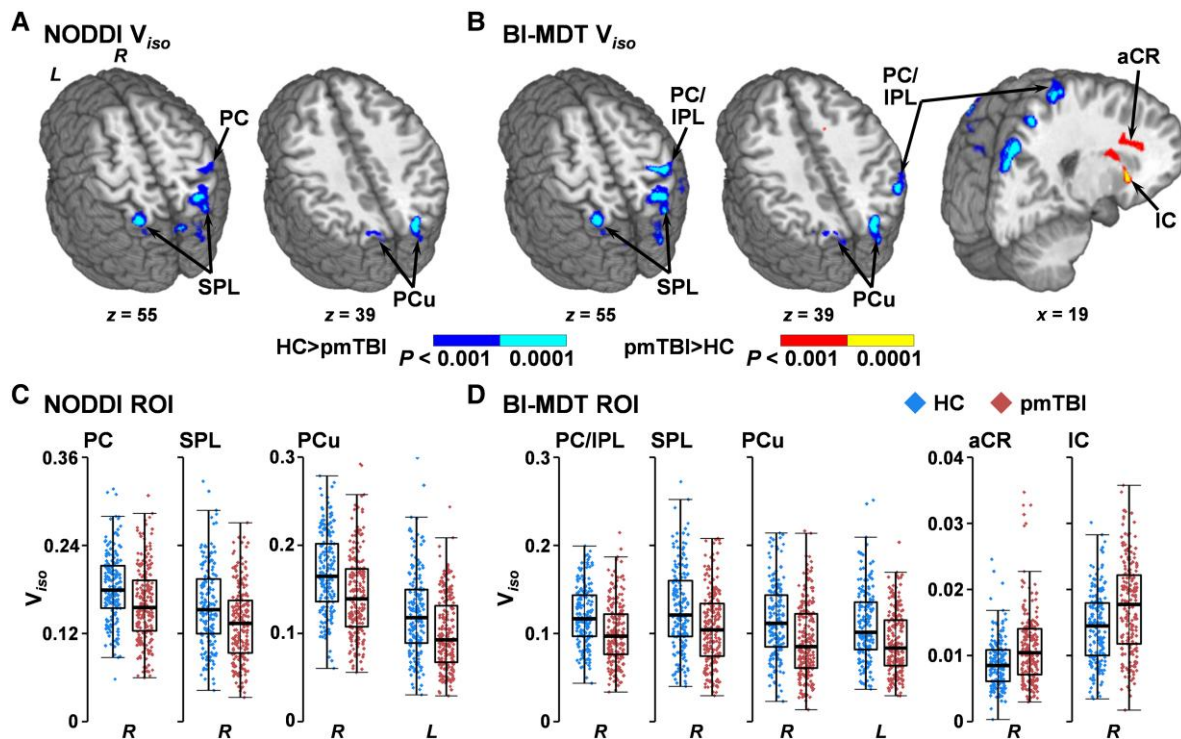


Figure 3 Voxel-wise analyses of V_{iso} . This figure presents the main effect of Group from analyses of isotropic volume fractions (V_{iso}) using either the standard NODDI algorithm (A and C) or a biologically informed MDT algorithm (BI-MDT; B and D). Data for patients with paediatric mild traumatic brain injury (pmTBI) (red diamonds) are plotted with warm colours in all panels, with HC (blue diamonds) data plotted with cool colours. Locations of sagittal (x) and axial (z) slices are given according to the Talairach atlas in the left (L) and (R) hemispheres. Both NODDI (A) and BI-MDT (B) indicated a main effect of group for regions of decreased V_{iso} (HC > pmTBI) in predominantly GM regions [post-central gyrus (PC), inferior (IPL) and superior (SPL) parietal lobule, precuneus (PCu)] for pmTBI relative to HC (dark blue: $P < 0.001$; cyan: $P < 0.0001$). In contrast, only the BI-MDT model was sensitive to regions of increased WM V_{iso} [anterior corona radiata (aCR) and the internal capsule (IC) extending into putamen] for pmTBI (red: $P < 0.001$; yellow: $P < 0.0001$). (C and D) Box-and-scatter plots [elements: median, interquartile range (IQR), and $3 \times$ IQR or local maxima/minima] for selected regions of interest (ROI) for each metric.

pmTBI group, with the presence of complicated pmTBI associated with increased ODI ($P = 0.003$). Sports-related injuries accounted for significant variance in FA ($P = 0.012$), V_{ic} ($P = 0.020$) and ODI ($P = 0.002$), whereas past history of pmTBI and PTA were not significant. Although our initial hypothesis was that clinical variables would not be associated with dMRI abnormalities, the 5P risk score was negatively associated with FA ($P = 0.007$) and positively associated with V_{ic} ($P = 0.005$), WM V_{iso} ($P = 0.020$) and ODI ($P = 0.002$). PCS severity did not account for significant variance. None of the injury severity variables were associated with decreased V_{iso} in GM.

Finally, supervised machine learning algorithms (random forests) investigated the diagnostic accuracy of the 5P risk score and Post-Concussion Symptom Inventory (Model 1), versus the diagnostic accuracy when weighted averages for FA, ODI, V_{ic} , GM V_{iso} and WM V_{iso} were included in the model (Model 2). Results from Model 1 indicated ~71.0% balanced diagnostic classification accuracy (sensitivity 73.4%, specificity 68.6%; Fig. 7), with the 5P score accounting for the greatest variance (11.4%). Classification accuracy increased up to 80.2% (sensitivity 82.0%, specificity 78.4%) when the five different patterns of dMRI abnormalities were included, although the 5P score maintained the highest variable importance score of 7.2%.

Discussion

Despite the large public health burden, our understanding of the pathophysiology of pmTBI remains relatively antiquated, with

diagnosis and prognosis primarily determined by symptom self-report.¹ Thus, even when youth accurately self-report symptoms, clinicians may not be able to detect any potential lingering physiological abnormalities that should principally inform care.⁶¹ Consistent with previous studies,^{14,15} current results provide additional evidence of DTI abnormalities (FA and MD) that persist up to 4 months post-injury, as well as tissue-dependent changes in free water volume fractions and increased intracellular volume. These diffusion abnormalities improved classification accuracy by ~10% even when controlling for current gold standards such as clinically derived risk scores and PCS.³ However, individual dMRI metrics only accounted for a few percentage points in terms of diagnostic accuracy, with all voxel-wise effect size maps in the small to medium range. Collectively, results suggest that dMRI abnormalities assessed in the current study are unlikely to be sufficient for accurate diagnosis of pmTBI when used in isolation.

A minority of participants self-endorsed significant PCS at both the SA (40.9%) and EC (21.9%) visits, even when applying a normative method that significantly reduces the number of false positives.⁵³ Small but significant deficits in attention and processing speed were present at the SA visit but showed evidence of full recovery, whereas residual cognitive deficits were present for verbal memory and executive functioning at 4 months. Previous studies have also reported continued cognitive deficits following pmTBI,^{62–66} although others have reported null results in both paediatric and adult samples.⁶⁷ Collectively, both current and previous findings suggest incomplete clinical recovery for a minority of

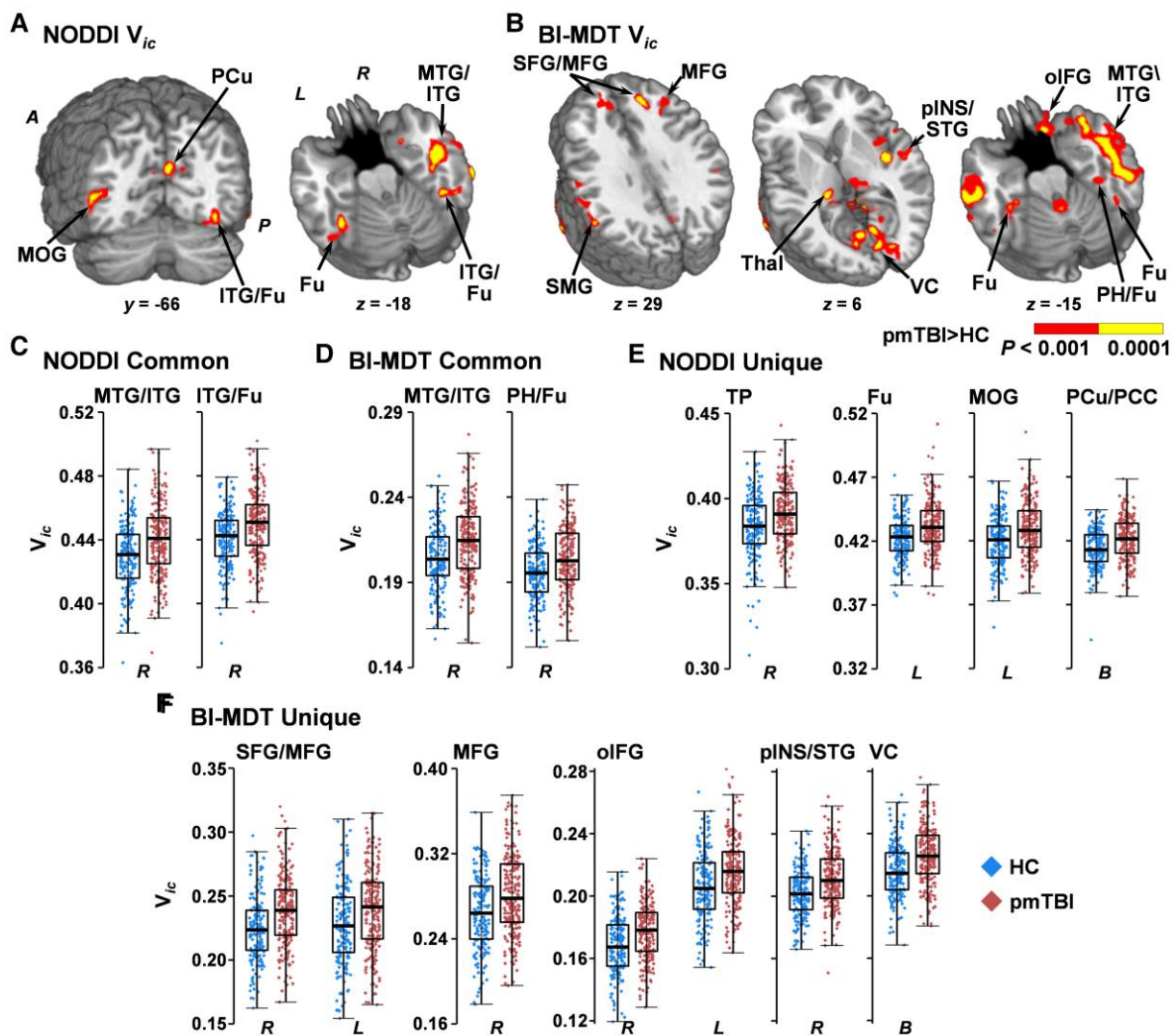


Figure 4 Voxel-wise analyses of V_{ic} . Results from analyses of V_{ic} using either the standard NODDI (A) or a biologically informed MDT algorithm (BI-MDT; B) for the main effect of Group. Locations of coronal (y) and axial (z) slices are given according to the Talairach atlas in anterior (A) and posterior (P) positions in the left (L) and (R) hemispheres. Both models demonstrated increased V_{ic} (red: $P < 0.001$; yellow: $P < 0.0001$) for patients with pmTBI (red diamonds) relative to HC (blue diamonds), although findings were more extensive in the biologically informed model. NODDI (C) and BI-MDT (D) box-and-scatter plots [elements: median, interquartile range (IQR) and $3 \times$ IQR or local maxima/minima] for common regions of interest, including the middle and inferior temporal gyrus (MTG/ITG) and the fusiform gyrus (Fu) extending into parahippocampal gyrus (PH) or ITG. (E) Exemplar regions unique to the NODDI algorithm including the temporal pole (TP), middle occipital gyrus (MOG) and bilateral (B) precuneus and posterior cingulate (PCu/PCC). (F) Exemplar regions unique to the BI-MDT algorithm, including superior and middle frontal gyrus (SFG/MFG), the MFG alone, orbital aspect of the inferior frontal gyrus (oIFG), posterior insula and superior temporal gyrus (pINS/STG) and visual cortex/cuneus (VC). There were many other significant regions of interest from the BI-MDT analysis (Supplementary material) that are displayed [e.g. supramarginal gyrus (SMG), thalamus (Thal)] but not plotted.

pmTBI patients up to 4 months post-injury across multiple domains, highlighting the need for multi-dimensional clinical assessments.⁶⁸

Similar to previous pmTBI studies, FA was increased^{12–16} and MD decreased.^{12,13,16} DTI abnormalities in the current sample were primarily limited to GM and persisted up to 4 months post-injury,^{14,15} suggesting that physiological recovery may require an extended period of time. Although other studies have reported null and contradictory results, a pattern of increased FA and reduced MD represents the most consistently reported DTI results in systematic reviews.^{1,6} Methodological (e.g. whole-brain versus region of interest versus tract-based analyses, use of different control groups) and statistical factors also probably contribute to disparities in findings across studies. Calculated voxel-wise effect size maps for the current study were typically in the small to

medium range (0.30–0.50), and cross-validation results indicated that larger samples ($\sim n = 120$ –140 per group) may be necessary to reliably detect differences.

One recent cross-sectional study⁶⁹ reported null findings when comparing DTI and NODDI volume fraction estimates in seven WM tracts in a large cohort of pmTBI relative to orthopaedically injured controls. In contrast, current findings from voxel-wise analyses indicated that intracellular volume fractions were increased for both GM and WM following pmTBI, whereas free water volume estimates varied as a function of tissue type (WM = increased; GM = decreased). Findings of decreased GM free water fractions and reduced MD were typically observed in the same regions,^{28,70} whereas differences in intracellular volume fractions were more widespread, occurred in both GM and WM and did not necessarily track with traditional DTI metrics. Similar to previous studies,^{29,71,72} the

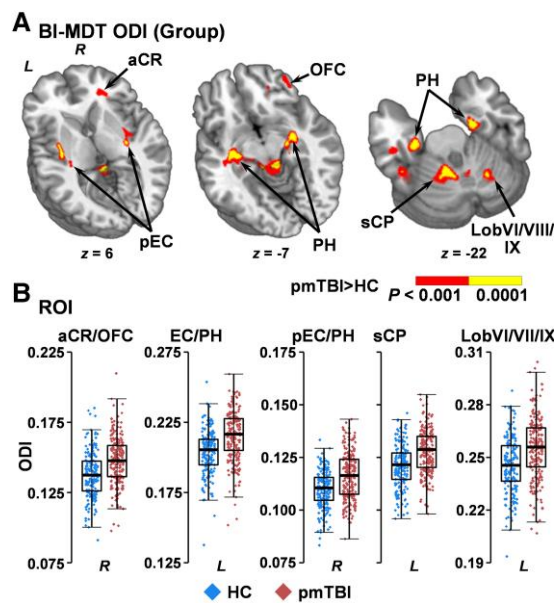


Figure 5 Voxel-wise analyses of ODI. Regions showing significantly (red: $P < 0.001$; yellow: $P < 0.0001$) increased ODI for patients with pmTBI (red diamonds) relative to HC (blue diamonds) using the biologically informed MDT algorithm (BI-MDT; A). Locations of sagittal (x) and axial (z) slices are given according to the Talairach atlas in the left (L) and (R) hemispheres. (B) Box-and-scatter plots [elements: median, interquartile range (IQR) and $3 \times$ IQR or local maxima/minima] for selected regions of interest, including the anterior corona radiata (aCR) extending through other WM tracts to orbitofrontal cortex (OFC), entire (EC) or only posterior (pEC) aspects of the external capsule extending into anterior insula and parahippocampal gyrus (PH), and superior cerebellar peduncle (sCP) extending into Lobules I–VI of the cerebellum.

sensitivity of multicompartamental volume estimates to group pathology appears to be higher than traditional DTI metrics. Previous adult studies have reported decreased intracellular volume fractions during SA mTBI^{27,29} as well as increased intracellular volume fractions in repetitive mTBI,²⁸ with either non-significant differences²⁷ or increased WM free water.^{28,29}

It has been suggested^{25,32} that the assumptions used in several geometric models^{30,31} are invalid. However, the impact of these assumptions on the detection of clinical pathology is unknown. Current results indicate that differentially modelling intra- and extracellular parallel diffusivities in a tissue-specific fashion fundamentally alters statistical relationships between diffusion metrics and potentially affects the clinical sensitivity of volume fraction estimates. Specifically, strong statistical relationships were observed between NODDI estimates of ODI and FA in healthy children and adults in current and previous studies,^{28,70} with other studies demonstrating NODDI volume estimates can be approximated from single-shell acquisitions at higher b -values.⁷³ In contrast, this relationship did not exist between FA and MDT estimates of ODI, and estimates of V_{ic} and ODI were statistically dissimilar across NODDI and MDT when intracellular and extracellular diffusivity values were altered in a tissue-dependent fashion to be more biologically plausible.^{25,32,33} The MDT model was also more sensitive to WM pathology for both free water and ODI estimates. These group differences in free water and ODI WM values were shown to be highly reproducible in our cross-validation analyses, and did not appear to be simply related to thresholding effects. Reproducibility analyses

also suggested that increased free water in WM was consistently observed in other tracts such as the cerebellar peduncles, but did not meet the necessary volume threshold for full family-wise error correction.

Although histopathological-imaging correlates exist for both DTI and multicompartamental models,^{74–77} there are no true gold standards for measuring cellular dysfunction with standard *in vivo*, human imaging. Exponential differences exist between imaged tissue volumes on a conventional scanner (e.g. typically 8μ) versus volumes represented by the intra/extracellular milieu for neurites (typically $1–8 \times 10^{-9} \mu$) and neurons. Most trauma-related changes to parenchymal microstructure will alter the rate of diffusion, with frequently cited pathologies including structural damage (e.g. changes in axonal membranes, dendrites or myelin), alterations in the net concentration of intraaxonal and extraaxonal water (cytotoxic or vasogenic oedema), and inflammatory processes.^{1,6} Critical to the field of trauma, the presence of tissue pathology (e.g. axonal beading, axonal swelling, oedema) both increases biological variability and fundamentally alters the assumptions that multicompartamental models use.^{25,72} These limitations caution against the strict interpretation of volume fraction estimates as being indicative of changes in ‘neurite density’ and ‘free water’ as is done in healthy tissue, and exponentially complicate the extrapolation to cellular pathology.^{74,78}

In light of these caveats, decreased GM free water and MD estimates could be indicative of a cytotoxic oedema as free water shifts from extracellular to intracellular compartments,⁷² although findings of increased FA have also previously been interpreted to be potentially indicative of a cytotoxic oedema.¹ Two recent studies reported increased intracellular and decreased free water fractions in affected relative to non-affected tissue in ischaemic stroke patients,^{72,79} where cytotoxic oedema has been more readily established as a known pathophysiology. In contrast, increased free water fractions has been interpreted to be indicative of vasogenic oedema due to blood–brain barrier leakage,^{29,71} which was only observed in WM in the current study when parallel diffusivity parameters were set to more biologically meaningful values. Similarly, the increased ODI observed in the current sample was also predominantly limited to WM, and suggests either structural pathology or vasogenic oedema resulting in more dispersion in neurites.

It is more challenging to interpret findings of increased intracellular volume following pmTBI. Although it is unlikely that there would be increased neurite density post-pmTBI, both trauma and secondary inflammatory processes are known to change the morphology of cellular substrates post-injury.^{80,81} Previous adult mTBI studies have also interpreted findings of decreased intracellular volume as being indicative of vasogenic oedema.^{27,29} Intracellular volume fractions have also been shown not to correlate with cortical thickness in patients with psychotic spectrum disorders,⁸² another putative measure of the density of neurites in GM. Thus, although current findings of increased V_{ic} and decreased V_{iso} have been reproduced across two forms of acquired brain injury,^{72,79} additional modelling and preclinical correlates are required to understand underlying microstructural correlates.

Previous work suggests that LOC/PTA is not predictive of functional and symptom-based outcomes in mTBI, especially at more chronic time points.^{83,84} Others have suggested that mTBI should be stratified into definitive, probable and possible categories based on LOC.⁸⁵ LOC and PTA have higher reliability and specificity relative to PCS,^{38,53,86} and have recently demonstrated a dose-dependent response for sport-related concussion severity in blood-based biomarker studies.^{87,88} Similar to previous studies,^{34,35} no

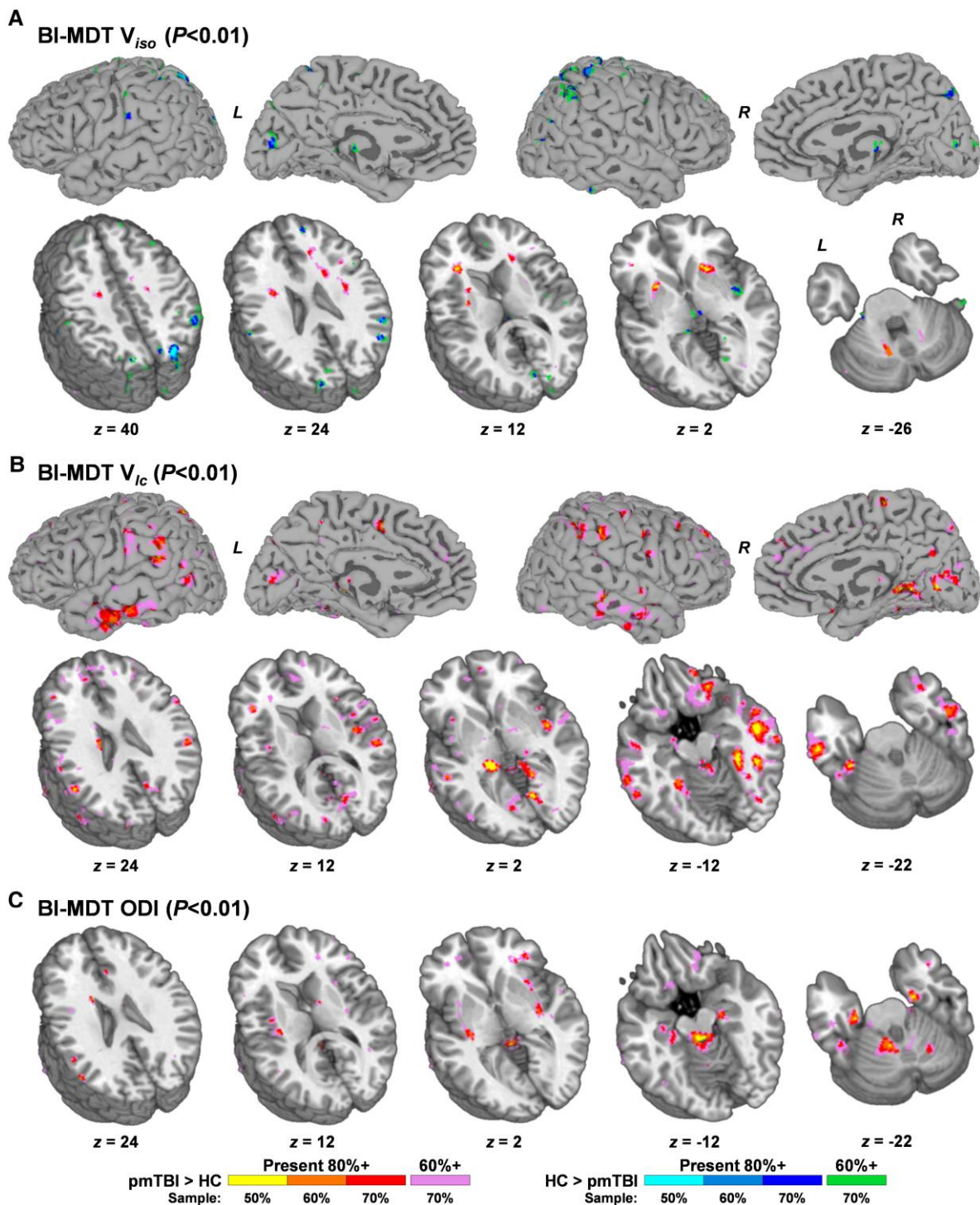


Figure 6 Cross-validation of multicompartmental model results. Results from cross-validation analyses of V_{iso} (A), V_{ic} (B) and ODI (C) data from the biologically informed MDT (BI-MDT) algorithm at 50, 60 and 70% of the total sample size (sampled without replacement; 300 iterations). For each metric, a statistical threshold (uncorrected $P < 0.01$) was applied to main effect of Group for each iteration on a voxel-wise basis. Active voxels were then summed across iterations and divided by the number of iterations to form percentage values. Voxels demonstrating main effects are colour-coded by both direction of effect (paediatric mild traumatic brain injury (pmTBI) > HC = warm; HC > pmTBI = cool) and level of reproducibility. In the first step, voxels were colour-coded for each sample size where a minimum of 80% reproducibility was achieved (50% of sample: yellow or cyan; 60% of sample: orange or middle blue; 70% of sample: red or dark blue). In the second step, voxels that achieved a minimum of 60% reproducibility at 70% of the total sample size were denoted (pink or green colours). Data are both projected to the surface and displayed for selected axial slices (z ; see Figs 3-5) according to the Talairach atlas for V_{ic} and V_{iso} , whereas results are presented in volume format only for ODI due to limited GM involvement.

significant relationships were observed between group-wise dMRI abnormalities and self-reported PCS, whereas LOC was associated with both changes in intracellular volume fractions and increased

WM free water. Both sport-related injuries and the presence of complicated pmTBI also accounted for significant unique variance in terms of dMRI abnormalities within pmTBI patients. Other

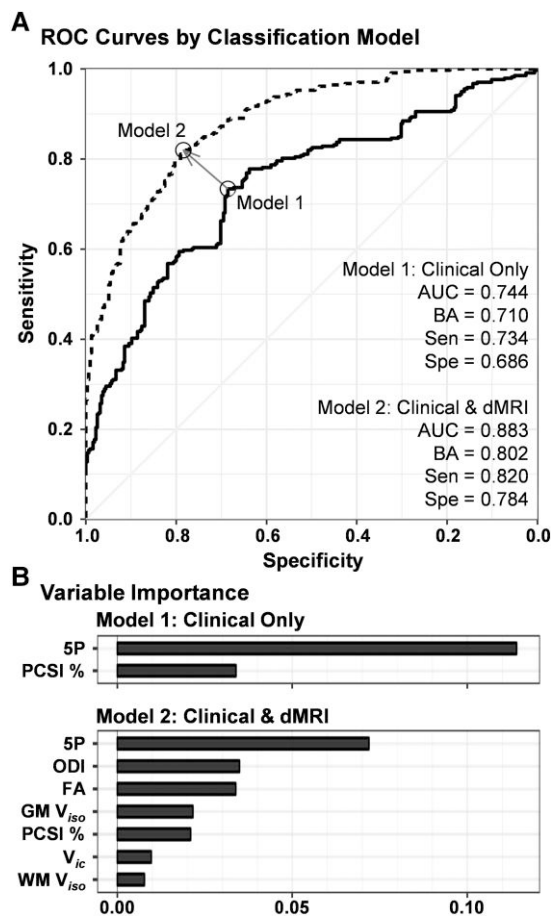


Figure 7 Group classification using random forest machine learning algorithm. (A) The receiver operating characteristics (ROC) results from the random forest supervised machine learning algorithm for classifying patients with paediatric mild traumatic brain injury (pmTBI) relative to HC. Two models compared diagnostic accuracy with current clinical gold standards [5P risk score (5P) and percentage of total possible score on the Post-Concussion Symptom Inventory (PCSA, %; solid line) or clinical gold standards plus significant dMRI findings (dashed line)]. dMRI variables included the weighted average of increased (pmTBI > HC) FA, decreased (HC > pmTBI) GM and increased WM V_{iso} , increased V_{ic} and increased ODI. All volume fraction estimates were obtained from the biologically informed MDT algorithm. Estimates for area under the curve (AUC), balanced accuracy (BA), sensitivity (Sen) and specificity (Spe) are provided for each model. (B) The variable importance for each metric in each model.

studies have reported decreased FA in the uncinate fasciculus²¹ and left middle frontal gyrus WM²³ when pmTBI with persistent symptoms were treated as a binary group. However, a large aggregate study ($n \approx 50\,000$) recently suggested that thousands of samples may be necessary to reliably observe brain-wide associations with complex psychological constructs such as cognition and behaviour,⁸⁹ which probably extrapolates to persistent PCS given its observed psychometric properties.⁵³ Contrary to *a priori* predictions, the 5P prediction rule³ was both associated with several dMRI abnormalities and had the highest diagnostic sensitivity/specificity during a supervised machine learning approach, even relative to PCS. Thus, current results indicate that diagnostic predictive accuracy of the 5P prediction rule should be evaluated in future biomarker pmTBI studies as well.

A frequently overlooked factor for pmTBI studies is the potential confounding effects of age-at-injury on emotion, cognition and brain

structure, all of which vary with biological sex and pubertal stage.^{10,11} Theories derived from preclinical models suggest improved outcomes in the very young due to increased plasticity following TBI,⁹⁰ although contrary evidence also exists for injuries occurring during critical periods.^{8,9,91} Age-at-injury was associated with increased self-reported PCS in the pmTBI group, but did not account for any additional variance in terms of diffusion abnormalities or cognitive dysfunction. These results therefore replicate adolescence as a risk factor for slower symptom-based recovery,³ but do not provide a clear physiological basis for this phenomenon from a microstructural perspective. Other pmTBI studies have also reported null findings in terms of age-at-injury for both diffusion⁹² and resting state metrics of regional homogeneity and low-frequency fluctuations in neural activity.⁹³

In contrast, another study¹¹ reported that middle childhood was associated with both greater injury and increased recovery on diffusion and structural imaging metrics relative to adolescents (less injury coupled with less recovery). Other clinical studies have indicated worse outcomes for children who were injured before 7 years of age,⁹⁴ as well as improved imaging outcomes in older adolescents with severe TBI.¹⁰ Several of these studies spanned the spectrum of injury severity and sampled at various time points post-injury, whereas the current study adopted a relatively homogenous sampling strategy both in terms of injury severity and acuity. Thus, current null findings for age-at-injury results may not generalize to more severe or chronically injured samples, or to children <8 years old. Studies on typical development have report increased FA and decreased MD in WM regions as a function of age,⁹⁵ along with complex, non-linear changes in cortical thickness, subcortical volumes, WM volumes and functional connectivity.^{96–98} Age-related microstructural changes include a combination of synaptic pruning of excessive connections in conjunction with increased myelination,⁹⁹ especially for prefrontal cortex. Larger sample sizes may therefore be required to detect any putative, complex interactions between age-at-injury and development trajectories on diffusion metrics. The current study may also not have sampled results over a sufficient period of time post-injury or in a broad enough cohort to detect age-at-injury effects. For example, age-at-injury effects could be more prevalent in younger samples (children <7 years of age),⁹⁴ or may express themselves over a longer period than the 4 months used in the current study.

Strengths of the current study include a large and homogenous sample with a high retention rate for follow-up visits (>80%). All data were collected at the same imaging centre and on the same machine, reducing concerns about inter-scanner and vendor-related differences in imaging signals that may overwhelm the smaller effect sizes associated with mild TBI.^{29,92,92,100} On the other hand, this single-centre approach also increased the risk of sampling bias and limits the generalization of findings. The former limitation was partially mitigated by our extensive cross-validation analyses, which demonstrated reproducible findings at ~70% of the total sample size. Second, most group differences on DTI metrics were observed in GM or grey/white junctions. Although animal studies suggest that diffusion sequences are capable of capturing GM microstructural changes, FA approaches the noise floor in GM and thus may be inherently less reliable.⁷⁵ Third, the current study did not include an orthopaedically injured control cohort, which may provide a better control for non-specific injury effects as well as potential differences in sampling strategies for imaging findings.¹⁰¹ Fourth, although our estimates of intra- and extracellular diffusivity were based on the literature,^{25,32,33} it is likely that these parameters will continue to evolve. Finally, although it is imperative to recognize limitations associated with deducing cellular

pathology from imaging metrics, a far more critical limitation for the field of concussion is the continued reliance on self-reported symptoms to both diagnose injury and prognose outcomes from both psychometric^{53,102} and tautological perspectives.

In summary, current dMRI findings provide corroboration of an incomplete clinical and pathophysiological recovery from pmTBI at 4 months post-injury and highlight the continued need for large, prospective studies on the physiological consequences of pmTBI.^{1,6} Effect size calculations, supervised machine learning classification algorithms and cross-validation results all indicate that the magnitude of these dMRI abnormalities are likely to be in the small to medium range. Current results suggest that novel multicompartamental models are more sensitive to putative pmTBI pathology and that sensitivity increased when using parameters that more accurately reflect diffusion in healthy tissue. However, current results also suggest that dMRI data in isolation may be insufficient to achieve a high degree of objective diagnostic accuracy in pmTBI. This finding is to be expected given known heterogeneities that exist for pathophysiology, mechanism of injury and even clinical definitions of pmTBI (7.1–98.7% classified as mTBI across 17 definitions).¹⁰² Similar to current clinical gold standards,³ multiple imaging, autonomic, neurosensory and blood-based biomarkers are likely to be necessary to fully understand the pathophysiological consequences of paediatric head trauma.¹⁰³

Funding

This research was supported by grants from the National Institutes of Health (<https://www.nih.gov>; grant numbers NIH 01 R01 NS098494-01A1, R01 NS098494-03S1A1 and P30 GM122734) to Andrew R. Mayer. The NIH had no role in study review, data collection and analysis, decision to publish or preparation of the manuscript.

Competing interests

The authors report no competing interests.

Supplementary material

[Supplementary material](#) is available at *Brain* online.

References

- Mayer AR, Kaushal M, Dodd AB, et al. Advanced biomarkers of pediatric mild traumatic brain injury: Progress and perils. *Neurosci Biobehav Rev*. 2018;94:149–165.
- Rausa VC, Anderson V, Babl FE, Takagi M. Predicting concussion recovery in children and adolescents in the emergency department. *Curr Neurol Neurosci Rep*. 2018;18:78.
- Zemek R, Barrowman N, Freedman SB, et al. Clinical risk score for persistent postconcussion symptoms among children with acute concussion in the ED. *JAMA*. 2016;315:1014–1025.
- Barkhoudarian G, Hovda DA, Giza CC. The molecular pathophysiology of concussive brain injury—An update. *Phys Med Rehabil Clin N Am*. 2016;27:373–393.
- Wang KK, Yang Z, Zhu T, et al. An update on diagnostic and prognostic biomarkers for traumatic brain injury. *Expert Rev Mol Diagn*. 2018;18:165–180.
- Schmidt J, Hayward KS, Brown KE, et al. Imaging in pediatric concussion: A systematic review. *Pediatrics*. 2018;141:e20173406.
- Mannix R, Levy R, Zemek R, et al. Fluid biomarkers of pediatric mild traumatic brain injury: A systematic review. *J Neurotrauma*. 2020;37:2029–2044.
- Kolb B, Mychasiuk R, Williams P, Gibb R. Brain plasticity and recovery from early cortical injury. *Dev Med Child Neurol*. 2011;53-(Suppl 4):4–8.
- Kolb B, Teskey GC. Age, experience, injury, and the changing brain. *Dev Psychobiol*. 2012;54:311–325.
- Dennis EL, Caeyenberghs K, Hoskinson KR, et al. White matter disruption in pediatric traumatic brain injury: Results from ENIGMA pediatric moderate to severe traumatic brain injury. *Neurology*. 2021;97:e298–e309.
- Ewing-Cobbs L, Johnson CP, Juranek J, et al. Longitudinal diffusion tensor imaging after pediatric traumatic brain injury: Impact of age at injury and time since injury on pathway integrity. *Hum Brain Mapp*. 2016;37:3929–3945.
- Babcock L, Yuan W, Leach J, Nash T, Wade S. White matter alterations in youth with acute mild traumatic brain injury. *J Pediatr Rehabil Med*. 2015;8:285–296.
- Borich M, Mekan N, Boyd L, Virji-Babul N. Combining whole-brain voxel-wise analysis with *in vivo* tractography of diffusion behavior after sports-related concussion in adolescents: A preliminary report. *J Neurotrauma*. 2013;30:1243–1249.
- Mayer AR, Ling JM, Yang Z, Pena A, Yeo RA, Klimaj S. Diffusion abnormalities in pediatric mild traumatic brain injury. *J Neurosci*. 2012;32:17961–17969.
- van Beek L, Vanderauwera J, Ghesquiere P, Lagae L, De SB. Longitudinal changes in mathematical abilities and white matter following paediatric mild traumatic brain injury. *Brain Inj*. 2015;29:1701–1710.
- Wilde EA, McCauley SR, Hunter JV, et al. Diffusion tensor imaging of acute mild traumatic brain injury in adolescents. *Neurology*. 2008;70:948–955.
- Friedman SD, Poliakov AV, Budech C, et al. GABA Alterations in pediatric sport concussion. *Neurology*. 2017;89:2151–2156.
- Maugans TA, Farley C, Altaye M, Leach J, Cecil KM. Pediatric sports-related concussion produces cerebral blood flow alterations. *Pediatrics*. 2012;129:28–37.
- Ware AL, Shukla A, Goodrich-Hunsaker NJ, et al. Post-acute white matter microstructure predicts post-acute and chronic post-concussive symptom severity following mild traumatic brain injury in children. *Neuroimage Clin*. 2020;25:102106.
- Guberman GI, Houde JC, Ptito A, Gagnon I, Descoteaux M. Structural abnormalities in thalamo-prefrontal tracks revealed by high angular resolution diffusion imaging predict working memory scores in concussed children. *Brain Struct Funct*. 2020;225:441–459.
- King R, Grohs MN, Kirton A, Lebel C, Esser MJ, Barlow KM. Microstructural neuroimaging of white matter tracts in persistent post-concussion syndrome: A prospective controlled cohort study. *Neuroimage Clin*. 2019;23:101842.
- Wu T, Merkle TL, Wilde EA, et al. A preliminary report of cerebral white matter microstructural changes associated with adolescent sports concussion acutely and subacutely using diffusion tensor imaging. *Brain Imaging Behav*. 2017;12:962–973.
- Mac Donald CL, Barber J, Wright J, et al. Longitudinal clinical and neuroimaging evaluation of symptomatic concussion in 10- to 14-year-old youth athletes. *J Neurotrauma*. 2019;36:264–274.
- Jarrah A, Braun M, Ahluwalia M, et al. Revisiting traumatic brain injury: From molecular mechanisms to therapeutic interventions. *Biomedicine*. 2020;8:389.
- Jelescu IO, Palombo M, Bagnato F, Schilling KG. Challenges for biophysical modeling of microstructure. *J Neurosci Methods*. 2020;344:108861.

26. Harms RL, Fritz FJ, Tobisch A, Goebel R, Roebroek A. Robust and fast nonlinear optimization of diffusion MRI microstructure models. *Neuroimage*. 2017;155:82–96.
27. Churchill NW, Caverzasi E, Graham SJ, Hutchison MG, Schweizer TA. White matter during concussion recovery: Comparing diffusion tensor imaging (DTI) and Neurite Orientation Dispersion and Density Imaging (NODDI). *Hum Brain Mapp*. 2019;40:1908–1918.
28. Mayer AR, Ling JM, Dodd AB, Meier TB, Hanlon FM, Klimaj SD. A prospective microstructure imaging study in mixed-martial artists using geometric measures and diffusion tensor imaging: Methods and findings. *Brain Imaging Behav*. 2017;11:698–711.
29. Palacios EM, Owen JP, Yuh EL, et al. The evolution of white matter microstructural changes after mild traumatic brain injury: A longitudinal DTI and NODDI study. *Sci Adv*. 2020;6:eaz6892.
30. Zhang H, Schneider T, Wheeler-Kingshott CA, Alexander DC. NODDI: practical in vivo neurite orientation dispersion and density imaging of the human brain. *Neuroimage*. 2012;61:1000–1016.
31. Fieremans E, Jensen JH, Helpert JA. White matter characterization with diffusional kurtosis imaging. *Neuroimage*. 2011;58:177–188.
32. Jelescu IO, Budde MD. Design and validation of diffusion MRI models of white matter. *Front Phys*. 2017;5:61.
33. Guerrero JM, Adluru N, Bendlin BB, et al. Optimizing the intrinsic parallel diffusivity in NODDI: An extensive empirical evaluation. *PLoS One*. 2019;14:e0217118.
34. Satchell EK, Friedman SD, Bompadre V, Poliakov A, Oron A, Jinguji TM. Use of diffusion tensor imaging in the evaluation of pediatric concussions. *Musculoskelet Sci Pract*. 2019;42:162–165.
35. Shapiro JS, Silk T, Takagi M, et al. Examining microstructural white matter differences between children with typical and those with delayed recovery two weeks post-concussion. *J Neurotrauma*. 2020;37:1300–1305.
36. Kay T, Harrington DE, Adams R, et al. Definition of mild traumatic brain injury. *J Head Trauma Rehabil*. 1993;8:86–87.
37. McCrory P, Meeuwisse WH, Aubry M, et al. Consensus statement on concussion in sport: The 4th international conference on concussion in sport held in Zurich, November 2012. *Br J Sports Med*. 2013;47:250–258.
38. Hergert DC, Sicard V, Stephenson DD, et al. Test-retest reliability of a semi-structured interview to aid in pediatric traumatic brain injury diagnosis. *J Int Neuropsychol Soc*. 2021;1–13.
39. WHO Group. The alcohol, smoking and substance involvement screening test (ASSIST): Development, reliability and feasibility. *Addiction*. 2002;97:1183–1194.
40. Gioia GA, Collins M, Isquith PK. Improving identification and diagnosis of mild traumatic brain injury with evidence: Psychometric support for the acute concussion evaluation. *J Head Trauma Rehabil*. 2008;23:230–242.
41. Gioia GA, Schneider JC, Vaughan CG, Isquith PK. Which symptom assessments and approaches are uniquely appropriate for paediatric concussion? *Br J Sports Med*. 2009;43:i13–i22.
42. Buysse DJ, Yu L, Moul DE, et al. Development and validation of patient-reported outcome measures for sleep disturbance and sleep-related impairments. *Sleep*. 2010;33:781–792.
43. Pilkonis PA, Choi SW, Reise SP, Stover AM, Riley WT, Cella D. Item banks for measuring emotional distress from the Patient-Reported Outcomes Measurement Information System (PROMIS®): Depression, anxiety, and anger. *Assessment*. 2011;18:263–283.
44. Farrar JT, Young JP Jr, LaMoreaux L, Werth JL, Poole RM. Clinical importance of changes in chronic pain intensity measured on an 11-point numerical pain rating scale. *Pain*. 2001;94:149–158.
45. Kriz PK, Stein C, Kent J, et al. Physical maturity and concussion symptom duration among adolescent ice hockey players. *J Pediatr*. 2016;171:234–239.
46. Kosinski M, Bayliss MS, Bjorner JB, et al. A six-item short-form survey for measuring headache impact: The HIT-6. *Qual Life Res*. 2003;12:963–974.
47. Goodman R. The strengths and difficulties questionnaire: A research note. *J Child Psychol Psychiatry*. 1997;38:581–586.
48. Prinz RJ, Foster S, Kent RN, O’Leary KD. Multivariate assessment of conflict in distressed and nondistressed mother-adolescent dyads. *J Appl Behav Anal*. 1979;12:691–700.
49. Varni JW, Seid M, Rode CA. The PedsQL™: Measurement model for the pediatric quality of life inventory. *Med Care*. 1999;37:126–139.
50. Beers SR, Wisniewski SR, Garcia-Filion P, et al. Validity of a pediatric version of the Glasgow outcome scale-extended. *J Neurotrauma*. 2012;29:1126–1139.
51. Derogatis LR, Fitzpatrick M. The SCL-90-R, the Brief Symptom Inventory, and the BSI-18. In: Maruish M, editor. *The use of psychological testing for treatment planning and outcomes assessment: Vol. 3: Instruments of adults*. 3rd edn, Erlbaum; 2004. p 1–41.
52. Zemek R, Osmond MH, Barrowman N. Predicting and preventing postconcussive problems in paediatrics (5P) study: Protocol for a prospective multicentre clinical prediction rule derivation study in children with concussion. *BMJ Open*. 2013;3:e003550.
53. Mayer AR, Stephenson DD, Dodd AB, et al. Comparison of methods for classifying persistent post-concussive symptoms in children. *J Neurotrauma*. 2020;37:1504–1511.
54. Denning JH. The efficiency and accuracy of the test of memory malingering trial 1, errors on the first 10 items of the test of memory malingering, and five embedded measures in predicting invalid test performance. *Arch Clin Neuropsychol*. 2012;27:417–432.
55. Mayer AR, Cohen DM, Wertz CJ, et al. Radiologic common data elements rates in pediatric mild traumatic brain injury. *Neurology*. 2020;94:e241–e253.
56. Smith SM, Jenkinson M, Woolrich MW, et al. Advances in functional and structural MR image analysis and implementation as FSL. *Neuroimage*. 2004;23(Suppl 1):S208–S219.
57. Cox R, Glen D. Efficient, robust, nonlinear, and guaranteed positive definite diffusion tensor estimation. In: Proceedings of the International Society for Magnetic Resonance and Medicine, 14th Scientific Meeting, Seattle, WA. 2006.
58. Cox R, Chen G, Glen DR, Reynolds RC, Taylor PA. FMRI clustering in AFNI: false-positive rates redux. *Brain Connectivity*. 2017;7:152–171.
59. Breiman L. Statistical modeling: The two cultures. *Stat Sci*. 2001;16:199–231.
60. Breiman L. Random forests. *Mach Learn*. 2001;45:5–32.
61. Kamins J, Bigler E, Covassin T, et al. What is the physiological time to recovery after concussion? A systematic review. *Br J Sports Med*. 2017;51:935–940.
62. Babikian T, McArthur D, Asarnow RF. Predictors of 1-month and 1-year neurocognitive functioning from the UCLA longitudinal mild, uncomplicated, pediatric traumatic brain injury study. *J Int Neuropsychol Soc*. 2013;19:145–154.
63. Beauchamp MH, Aglipay M, Yeates KO, et al. Predictors of neuropsychological outcome after pediatric concussion. *Neuropsychology*. 2018;32:495–508.
64. Iverson GL, Brooks BL, Collins MW, Lovell MR. Tracking neuropsychological recovery following concussion in sport. *Brain Inj*. 2006;20:245–252.
65. McGrath N, Dinn WM, Collins MW, Lovell MR, Elbin RJ, Kontos AP. Post-exertion neurocognitive test failure among student-athletes following concussion. *Brain Inj*. 2013;27:103–113.

66. Rieger BP, Lewandowski LJ, Callahan JM, et al. A prospective study of symptoms and neurocognitive outcomes in youth with concussion vs orthopaedic injuries. *Brain Inj.* 2013;27:169–178.
67. Moore RD, Kay JJ, Ellemberg D. The long-term outcomes of sport-related concussion in pediatric populations. *Int J Psychophysiol.* 2018;132(Pt A):14–24.
68. Polinder S, Cnossen MC, Real RGL, et al. A multidimensional approach to post-concussion symptoms in mild traumatic brain injury. *Front Neurol.* 2018;9:1113.
69. Shukla A, Ware AL, Guo S, et al. Examining brain white matter after pediatric mild traumatic brain injury using neurite orientation dispersion and density imaging: An A-CAP study. *Neuroimage Clin.* 2021;32:102887.
70. Hanlon FM, Dodd AB, Ling JM, et al. The clinical relevance of gray matter atrophy and microstructural brain changes across the psychosis continuum. *Schizophr Res.* 2021;229:12–21.
71. Mayer AR, Quinn DK, Master CL. The spectrum of mild traumatic brain injury: A review. *Neurology.* 2017;89:623–632.
72. Wang Z, Zhang S, Liu C, et al. A study of neurite orientation dispersion and density imaging in ischemic stroke. *Magn Reson Imaging.* 2019;57:28–33.
73. Fukutomi H, Glasser MF, Murata K, et al. Diffusion tensor model links to neurite orientation dispersion and density imaging at high b-value in cerebral cortical gray matter. *Sci Rep.* 2019;9:12246.
74. Jelescu IO, Zurek M, Winters KV, et al. In vivo quantification of demyelination and recovery using compartment-specific diffusion MRI metrics validated by electron microscopy. *Neuroimage.* 2016;132:104–114.
75. Holleran L, Kim JH, Gangolli M, et al. Axonal disruption in white matter underlying cortical sulcus tau pathology in chronic traumatic encephalopathy. *Acta Neuropathol.* 2017;133:367–380.
76. Sato K, Kerever A, Kamagata K, et al. Understanding microstructure of the brain by comparison of Neurite Orientation Dispersion and Density Imaging (NODDI) with transparent mouse brain. *Acta Radiol Open.* 2017;6:2058460117703816.
77. Seppehrband F, Clark KA, Ullmann JF, et al. Brain tissue compartment density estimated using diffusion-weighted MRI yields tissue parameters consistent with histology. *Hum Brain Mapp.* 2015;36:3687–3702.
78. Lampinen B, Szczepankiewicz F, Martensson J, van Westen D, Sundgren PC, Nilsson M. Neurite density imaging versus imaging of microscopic anisotropy in diffusion MRI: A model comparison using spherical tensor encoding. *Neuroimage.* 2017;147:517–531.
79. Adluru G, Gur Y, Anderson JS, Richards LG, Adluru N, DiBella EV. Assessment of white matter microstructure in stroke patients using NODDI. In: *Proceedings of the 36th Annual International Conference of the IEEE. Engineering in Medicine and Biology Society.* 2014:742–745.
80. Budde MD, Janes L, Gold E, Turtzo LC, Frank JA. The contribution of gliosis to diffusion tensor anisotropy and tractography following traumatic brain injury: Validation in the rat using Fourier analysis of stained tissue sections. *Brain.* 2011;134(Pt 8):2248–2260.
81. Xu S, Zhuo J, Racz J, et al. Early microstructural and metabolic changes following controlled cortical impact injury in rat: A magnetic resonance imaging and spectroscopy study. *J Neurotrauma.* 2011;28:2091–2102.
82. Nazeri A, Mulsant BH, Rajji TK, et al. Gray matter neuritic microstructure deficits in schizophrenia and bipolar disorder. *Biol Psychiatry.* 2017;82:726–736.
83. McNally KA, Bangert B, Dietrich A, et al. Injury versus noninjury factors as predictors of postconcussive symptoms following mild traumatic brain injury in children. *Neuropsychology.* 2013;27:1–12.
84. van der Naalt J, Timmerman ME, de Koning ME, et al. Early predictors of outcome after mild traumatic brain injury (UPFRONT): An observational cohort study. *Lancet Neurol.* 2017;16:532–540.
85. Kutcher JS, Giza CC. Sports concussion diagnosis and management. *Continuum (Minneapolis).* 2014;20(6 Sports Neurology):1552–1569.
86. Iverson GL, Silverberg ND, Mannix R, et al. Factors associated with concussion-like symptom reporting in high school athletes. *JAMA Pediatr.* 2015;169:1132–1140.
87. McCrea M, Broglio SP, McAllister TW, et al. Association of blood biomarkers with acute sport-related concussion in collegiate athletes: Findings from the NCAA and department of defense CARE consortium. *JAMA Netw Open.* 2020;3:e1919771.
88. Meier TB, Huber DL, Bohorquez-Montoya L, et al. A prospective study of acute blood-based biomarkers for sport-related concussion. *Ann Neurol.* 2020;87:907–920.
89. Marek S, Tervo-Clemmens B, Calabro FJ, et al. Reproducible brain-wide association studies require thousands of individuals. *Nature.* 2022;603:654–660.
90. Kennard MA. Cortical reorganization of motor function: Studies on series of monkeys of various ages from infancy to maturity. *Arch Neurol Psychiatry.* 1942;48:227–240.
91. Anderson V, Spencer-Smith M, Leventer R, et al. Childhood brain insult: can age at insult help us predict outcome? *Brain.* 2009;132(Pt 1):45–56.
92. Goodrich-Hunsaker NJ, Abildskov TJ, Black G, et al. Age- and sex-related effects in children with mild traumatic brain injury on diffusion magnetic resonance imaging properties: A comparison of voxelwise and tractography methods. *J Neurosci Res.* 2018;96:626–641.
93. Stephenson DD, Meier TB, Pabbathi RS, et al. Resting-state power and regional connectivity after pediatric mild traumatic brain injury. *J Magn Reson Imaging.* 2020;52:1701–1713.
94. Anderson V, Moore C. Age at injury as a predictor of outcome following pediatric head injury: A longitudinal perspective. *Child Neuropsychol.* 1995;1:187–202.
95. Lebel C, Treit S, Beaulieu C. A review of diffusion MRI of typical white matter development from early childhood to young adulthood. *NMR Biomed.* 2019;32:e3778.
96. Paus T. Maturation of structural and functional connectivity in the human brain. In: Jirsa V and McIntosh AR, eds. *Handbook of brain connectivity.* Springer; 2007: 463–475.
97. Lenroot RK, Gogtay N, Greenstein DK, et al. Sexual dimorphism of brain developmental trajectories during childhood and adolescence. *Neuroimage.* 2007;36:1065–1073.
98. Power JD, Barnes KA, Snyder AZ, Schlaggar BL, Petersen SE. Spurious but systematic correlations in functional connectivity MRI networks arise from subject motion. *Neuroimage.* 2012;59:2142–2154.
99. Gennatas ED, Avants BB, Wolf DH, et al. Age-related effects and sex differences in gray matter density, volume, mass, and cortical thickness from childhood to young adulthood. *J Neurosci.* 2017;37:5065–5073.
100. Fortin JP, Parker D, Tunc B, et al. Harmonization of multi-site diffusion tensor imaging data. *Neuroimage.* 2017;161:149–170.
101. Wilde EA, Ware AL, Li X, et al. Orthopedic injured versus uninjured comparison groups for neuroimaging research in mild traumatic brain injury. *J Neurotrauma.* 2019;36:239–249.
102. Crowe LM, Hearps S, Anderson V, et al. Investigating the variability in mild traumatic brain injury definitions: A prospective cohort study. *Arch Phys Med Rehabil.* 2018;99:1360–1369.
103. Mayer AR, Quinn DK. Neuroimaging biomarkers of new-onset psychiatric disorders following traumatic brain injury. *Biol Psychiatry.* 2022;91:459–469.